Supplementary Information

Specificity of synaptic connectivity between layer 1 inhibitory interneurons and layer 2/3 pyramidal neurons in the rat neocortex

Christian Wozny[1] & Stephen R. Williams[1,2]

[1] MRC Laboratory of Molecular Biology,

Hills Road,

Cambridge

CB2 0QH, UK

Phone: +44 1223 252998

Fax: +44 1223 402310

[2] The Queensland Brain Institute

St Lucia, QLD 4072, Australia

Phone: +61 7 3346 6352

Fax: +61 7 3346 6301

Corresponding authors:

Stephen R. Williams srw@uq.edu.au

Christian Wozny cwozny@mrc-lmb.cam.ac.uk

Supplementary Figure 1

A, Reconstruction of a L2/3 pyramidal neuron. Please note axon collaterals in L1. ***B***, Twenty L2/3 pyramidal neurons were randomly selected for further analysis of the intrinsic properties. In line with previously published data (Larkum et al., 2007; Waters et al., 2003; Higgs and Spain, 2009) L2/3 pyramidal neurons had an average resting membrane potential of –76.5 ± 1.1 mV and an input resistance of 46 ± 3 MΩ and exhibited prominent rectification of the voltage – current relationship (Sutor and Zieglgansberger, 1987). ***C***, Averaged voltage-current relationship for twenty L2/3 pyramidal neurons. ***D***, Action potential firing frequency plotted against number of action potentials (events), highlighting the presence of spike frequency accommodation (same neurons as shown in ***A*** and ***B***).

Supplementary Figure 2

A, NGFC showing anatomical characteristics of short dendrites and large and dense axonal arbor, which is in this case, confined to L1 (as were five of the twelve successfully stained cells). ***B***, Example of c-AC neuron with one descending axon innervating deeper layers.

Supplementary Figure 3

A, Confocal image of a simultaneously recorded L1 neuron and L2/3 pyramidal neuron. L1 interneuron closed to L1-L2 boarder was characterized as chandelier cell, exhibiting several hundred vertically oriented axonal segments (enlarged in ***B***).

Supplementary Figure 4

A, Relationship between action potential firing frequency and injected current (f-I) for all FS cells. The f-I of anatomically identified Chandelier cells are shown in bold (n = 4). ***B***, Typical action potential firing pattern of a FS cell at the threshold from repetitive firing. ***C1*** Threshold firing pattern of a Chandelier cell, note the Chandelier cell shows shuttering firing behavior. ***C2*** High-frequency firing of the same Chandelier cell evoked by a larger positive current step.

Supplementary Figure 5

Bar diagram of the decay time constant of L2/3 Pyr-L1 uEPSPs. Significant differences indicated by stars (* $P < 0.05$, *** $P < 0.001$).

Supplementary Figure 6

A-C, Bar diagram of the basic properties of L1-L2/3 Pyr uIPSPs. Depending on the presynaptic cell type, differences were observed in the latency ***(A)***, rise time ***(B)***, half width (***C***) of uIPSPs. Significant differences indicated by stars (* $P < 0.05$, ** $P < 0.01$, *** $P < 0.001$).

Supplementary Figure 7

A, Chandelier cells selectively innervate the axon initial segment of a pyramidal neuron. Small arrows indicate putative synaptic boutons on the axon initial segment of the filled L2/3 pyramidal neuron, open arrows point to a neighboring axonal segment of the chandelier cell and the larger arrow indicates the first axonal branching point of the L2/3 axon. ***B***, Synaptically coupled Chandelier cell (upper trace) to layer 2/3 pyramidal neuron (lower trace) pair. The histogram shows the tight latency distribution of uIPSPs. ***C***, Synaptic responses are depolarizing at -62 mV, a potential at which, for example, NGFC-L2/3 pyramidal cell pairs showed hyperpolarizing uIPSPs (see Figure 7). Unitary IPSPs were blocked with $GABA_A$-receptor antagonist SR 95531 (2 μM).

Supplementary Figure 8

A, Voltage – current relationship for two BS cells. ***B***, Synaptically coupled BS-BS cell pair. ***C***, Unitary IPSPs at different membrane potential reveal reversal potential close to estimated GABA reversal potential (-65 mV).

References

1. Higgs MH, Spain WJ (2009) Conditional bursting enhances resonant firing in neocortical layer 2-3 pyramidal neurons. J Neurosci 29: 1285-1299.

2. Larkum ME, Waters J, Sakmann B, Helmchen F (2007) Dendritic spikes in apical dendrites of neocortical layer 2/3 pyramidal neurons. J Neurosci 27: 8999-9008.

3. Sutor B, Zieglgansberger W (1987) A low-voltage activated, transient calcium current is responsible for the time-dependent depolarizing inward rectification of rat neocortical neurons in vitro. Pflugers Arch 410: 102-111.

4. Waters J, Larkum M, Sakmann B, Helmchen F (2003) Supralinear Ca2+ influx into dendritic tufts of layer 2/3 neocortical pyramidal neurons in vitro and in vivo. J Neurosci 23: 8558-8567.

Supplementary Figure 1

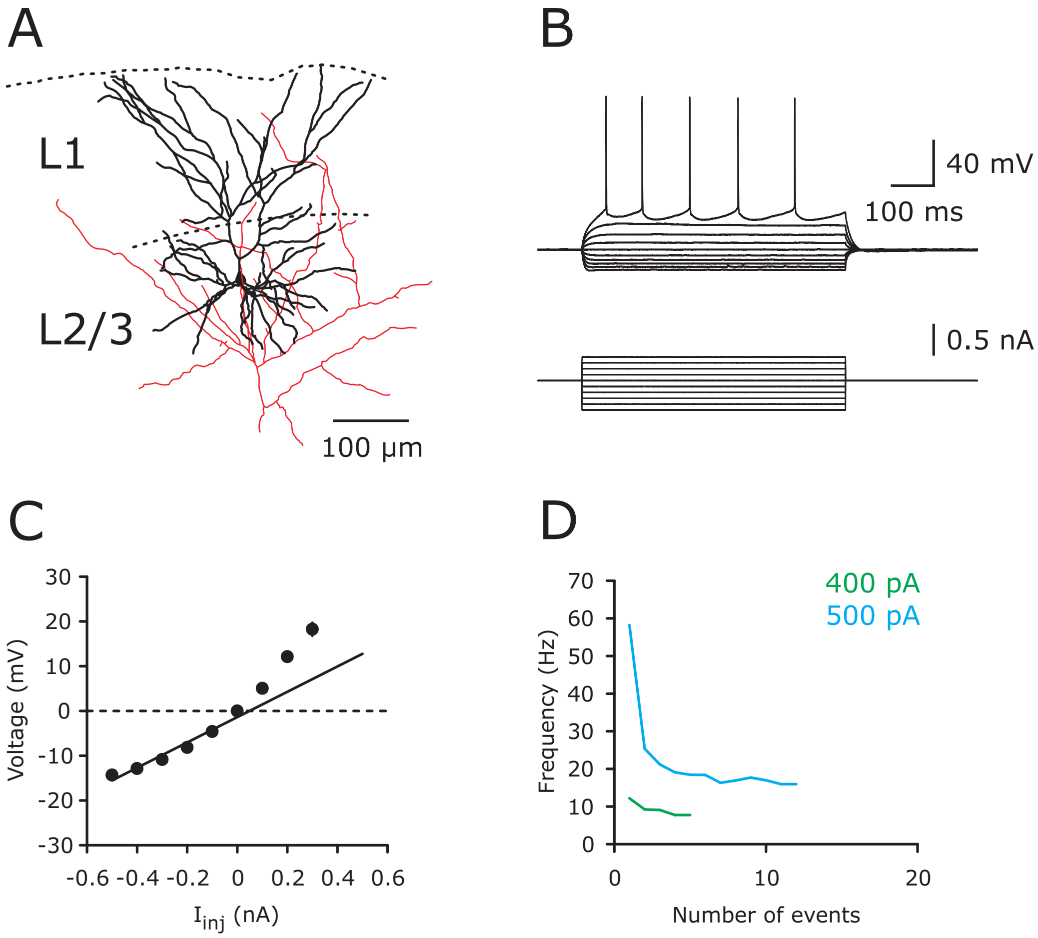

Supplementary Figure 2

A

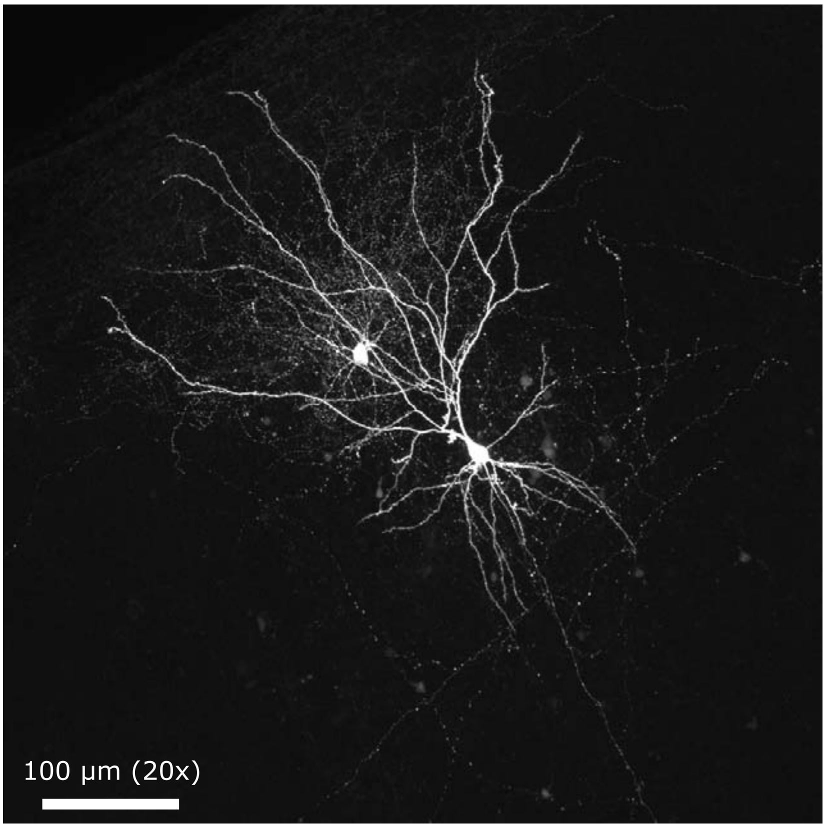

B

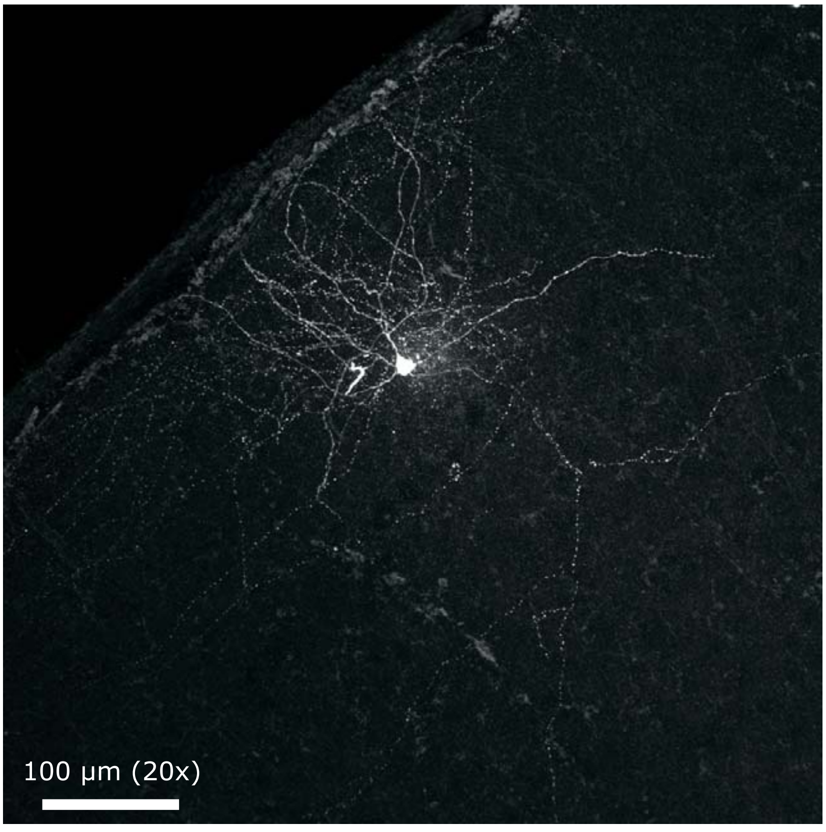

Supplementary Figure 3

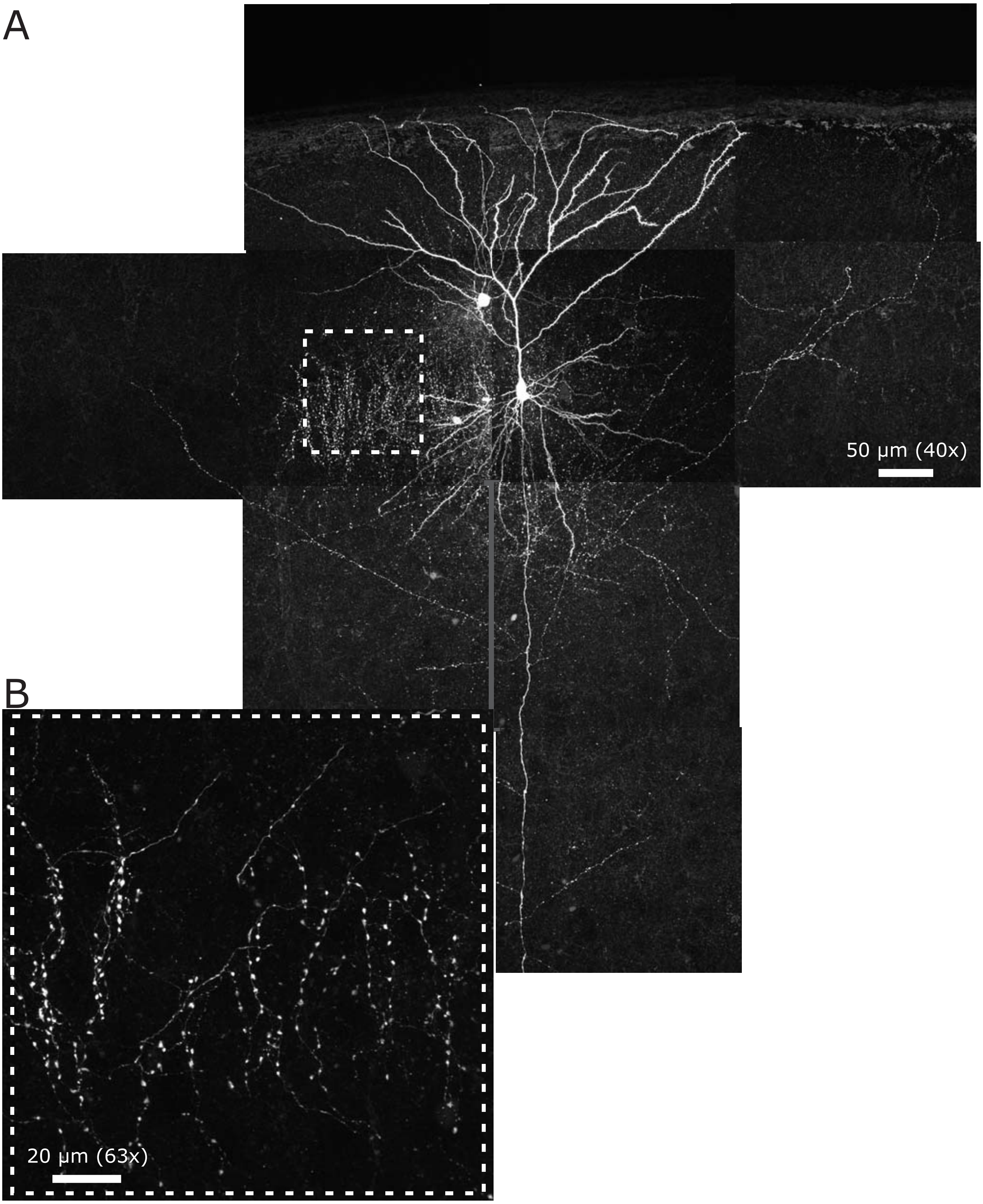

Supplementary Figure 4

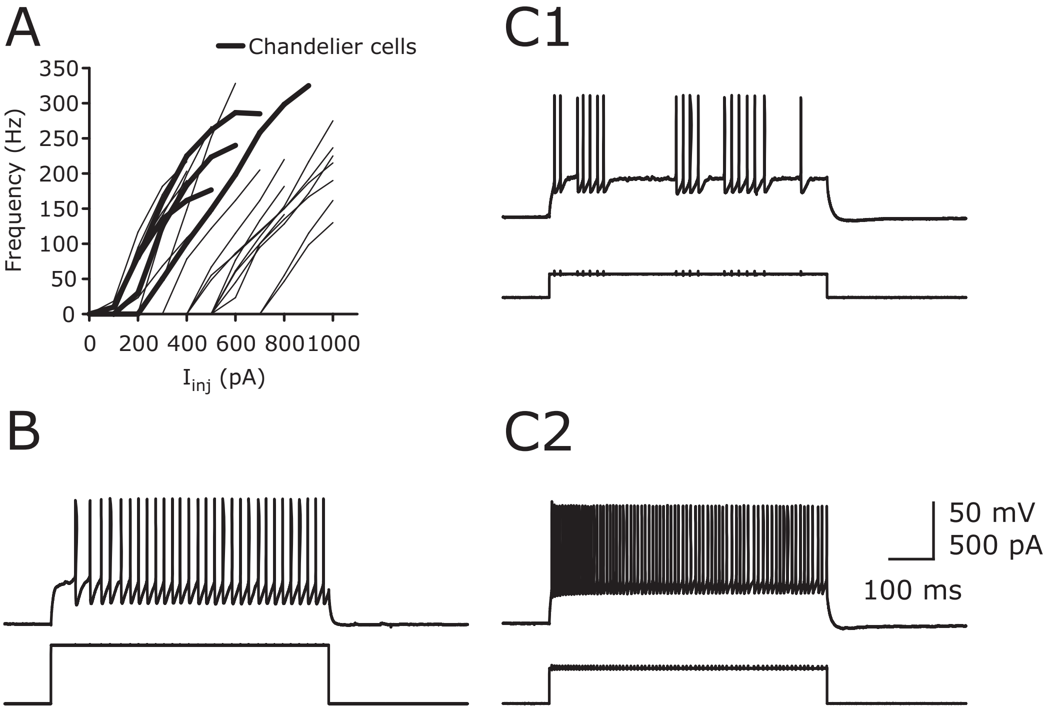

Supplementary Figure 5

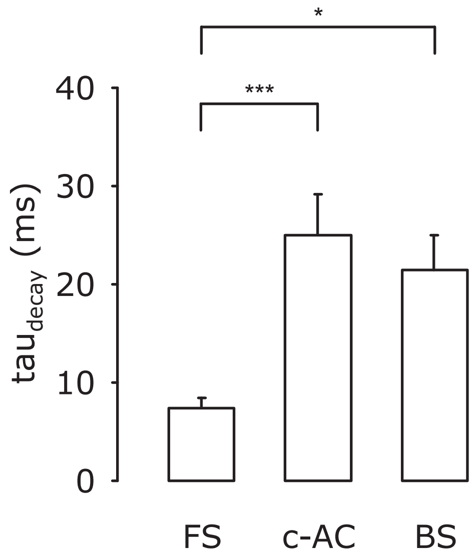

Supplementary Figure 6

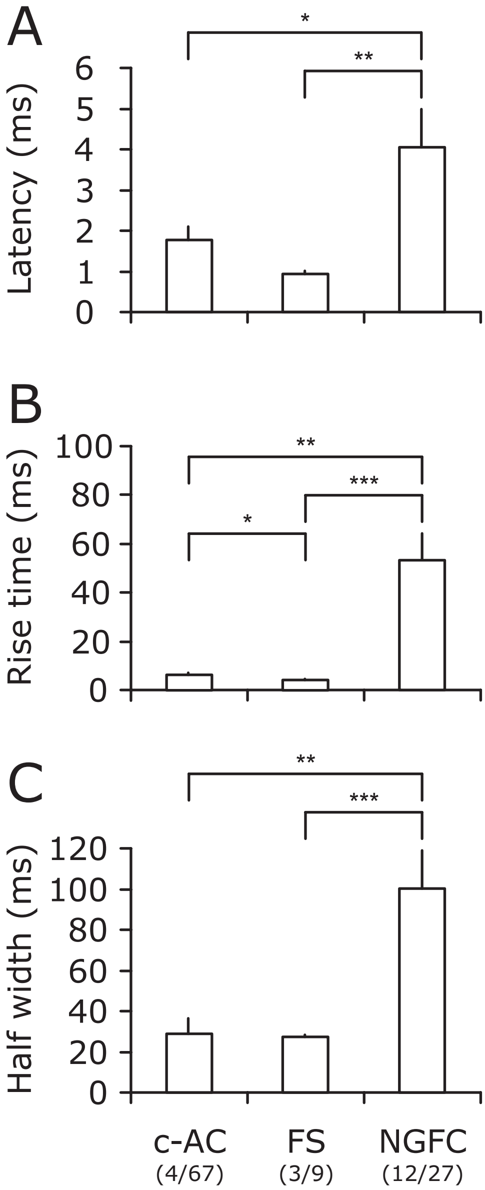

Supplementary Figure 7

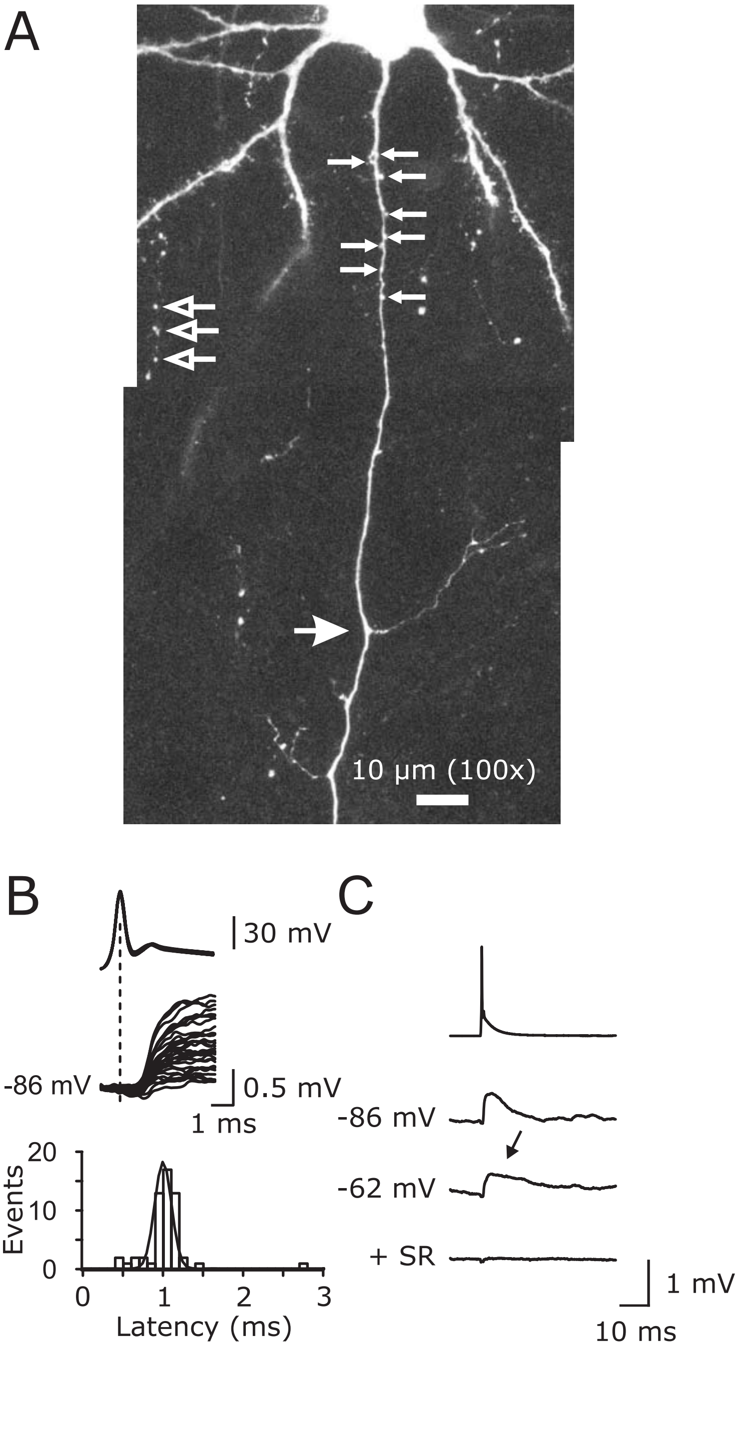

Supplementary Figure 8